

Theoretical description and experimental detection of the interference between parametric X radiation and coherent bremsstrahlung

V. V. Morokhovskiy, J. Freudenberger, and H. Genz

Institut für Kernphysik, Technische Universität Darmstadt, Schlossgartenstrasse 9, D-64289 Darmstadt, Germany

V. L. Morokhovskii

Institut für Kernphysik, Technische Universität Darmstadt, Schlossgartenstrasse 9, D-64289 Darmstadt, Germany and Kharkiv Institute of Physics and Technology, 61108 Kharkiv, Ukraine

A. Richter*

Institut für Kernphysik, Technische Universität Darmstadt, Schlossgartenstrasse 9, D-64289 Darmstadt, Germany and Wissenschaftskolleg zu Berlin, Wallotstrasse 19, D-14193 Berlin, Germany

J. P. F. Sellschop

Schonland Centre, University of the Witwatersrand, 2050 Johannesburg, South Africa

(Received 12 May 1999)

Parametric X radiation (PXR) produced by electrons with an energy of $E_0=4$ MeV interacting with the atoms in the (220) plane of a 20- μm silicon and a 55- μm diamond crystal and observed at an angle of 44° by a Si(Li) detector has been investigated with respect to the interference with coherent bremsstrahlung (CB) that originates in the same interaction process between the incoming relativistic electron and the crystal. Since the energy of PXR and CB is identical, contributions of both types of radiation are indistinguishable. The newly derived analytical expressions describe the radiation which consists of a coherent superposition of PXR and CB. For the comparison of the experimental results with the theoretical predictions a Monte Carlo simulation taking into account all effects accompanying the radiation process has been performed. The comparison shows very good agreement between experiment and theory.

I. INTRODUCTION

The interaction between a relativistic charged particle and a crystal causes besides other processes the generation of coherent X radiation. Due to the interaction between the relativistic particle and the charged particles composing a crystal both the particle itself and the crystal electrons become sources of coherent radiation. The radiation produced by the particle itself is called coherent bremsstrahlung (CB), while the radiation produced by the crystal electrons is known as parametric X radiation (PXR) or coherent polarization bremsstrahlung. The energy of both types of radiation \mathcal{E}_{ph} is determined by the periodicity of the crystal along the particle trajectory and is identical in both cases,¹⁻³

$$\mathcal{E}_{ph} = \frac{\hbar(\vec{g} \cdot \vec{v})}{1 - (\vec{v} \cdot \hat{k})/c^*}, \quad (1)$$

where \vec{g} is the reciprocal-lattice vector, corresponding to the crystal plane producing the radiation, \vec{v} is the particle velocity, and \hat{k} a unit vector pointing into the direction of observation; c^* represents the velocity of light in the crystal medium. Although having the same photon energy PXR and CB exhibit different angular distributions. Since CB is radiated by the relativistic particle itself its main intensity is concentrated within a cone of $1/\gamma$ in the forward direction, where γ represents the relativistic Lorentz factor. In contrast, the PXR reflex is emitted near the so-called "Bragg direction." It can be emitted at an arbitrary direction depending on the crystal orientation. At low particle energies, as considered in the

present paper, the angular extension of the PXR reflex amounts to approximately $5/\gamma$. Under specific experimental conditions both types of radiation can be observed simultaneously, and since they originate from the same interaction process they might interfere. The purpose of the present article is to investigate this interference effect theoretically and experimentally.

Although this subject was investigated before³⁻⁶ the theoretical descriptions of the phenomena are contradictory to each other, they are based on different formulas, do have different signs for the interference effect and are partially not reproducible and since the experimental data of Ref. 4 are compared only with the predictions of Ref. 4 it is not possible to decide whether one or the other of theoretical explanations is valid. Furthermore, since the theoretical expression of Ref. 4 cannot be reproduced and since the predictions for PXR only are not in agreement with our calculations the experimental findings quoted in Ref. 4 may be completely fortuitous. We therefore present in this work an independent derivation yielding different theoretical expressions describing the interference phenomena as well as an interesting experimental investigation of the process.

II. THEORETICAL CONSIDERATION

The theoretical description is based on the following assumptions which are in accordance with the experimental conditions of the present work as well as of all other experimental results mentioned in this paper: The motion of the

relativistic particle is described within the frame of the classical relativistic theory. Applying the classical theory is valid because the de Broglie wavelength of the relativistic particle is much smaller than the crystal constant ($2\pi\hbar/p \ll a$). Furthermore, it is assumed that the incoming charged particle does not occupy bound states within the potential of crystal planes and axes. The influence of the generated radiation on the motion of the particle will be neglected because the momentum of the relativistic particle is much larger than the momentum of the radiated photon ($p \gg k$). This approximation allows us to apply classical electrodynamics for the description of the radiation process. Finally, the interaction of the produced radiation with the crystal will not be taken into account, which has been termed kinematical principle.¹⁻³ It will also be assumed that the trajectory of the particle within the crystal represents a chain of straight segments, the length of which is smaller than the absorption length for the radiated photons in the crystal. This condition allows us to consider the photoabsorption for the radiated photons separately. To simplify the formulas, the average dielectric susceptibility of the crystal will be neglected ($\bar{\chi} = 0$). In this approach^{1,2} the average dielectric constant $\bar{\epsilon} = 1$ and the velocity of light in the crystal is equal to the velocity of light in vacuum ($c^* = c$). For further simplification, crystals consisting of one sort of atom only, i.e., monoatomic crystals, will be considered.

A. Parametric X radiation

Assuming that the trajectory of the relativistic particle inside the crystal is approximated by straight segments all theoretical considerations can be performed for such segment only. Later on it will be shown that the intensity of the coherent radiation is proportional to the length of a segment [see Eq. (13)]. Thus the total production rate does not depend on the division of the trajectory into such segments and is proportional to the crystal thickness. The charged particles composing a crystal experience a Coulomb force due to the interaction with the incoming relativistic particle. They are accelerated and thus radiate electromagnetic waves. Since the nuclei are much heavier than the electrons their contribution to the radiation produced can be neglected in all cases. So, PXR is produced solely by the electrons of a crystal. Denoting the electron charge density in the crystal by $\rho_e(\vec{r}) = -e_0 n_e(\vec{r})$, (see Fig. 1) where e_0 is the magnitude of the elementary charge and $n_e(\vec{r})$ the electron density, the force applied to a small volume of the electron charge distribution dV is equal to

$$\delta\vec{F}(t') = -e_0 \vec{E}(\vec{r}, t') n_e(\vec{r}) dV, \quad (2)$$

where $\vec{E}(\vec{r}, t')$ is the Coulomb field of the relativistic particle:⁷

$$\vec{E}(\vec{r}, t') = \frac{ze_0 \vec{r}'}{\gamma^2 r'^3 \left(1 - \frac{v^2}{c^2} \sin^2 \vartheta\right)^{3/2}}. \quad (3)$$

The charge number of the relativistic particle is denoted by z (for electrons $z = -1$), $r' = |\vec{r}'|$ and ϑ are defined in Fig. 1.

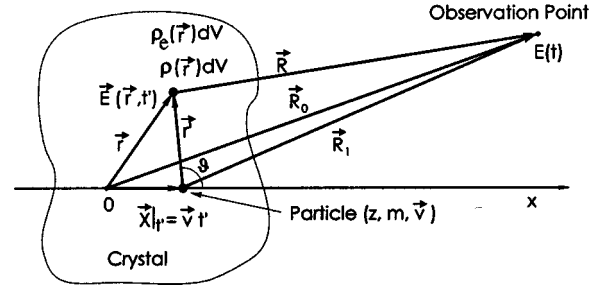


FIG. 1. Definition of variables. A relativistic particle is moving with a velocity \vec{v} along the x axis. The electromagnetic waves, reaching the observation point at time t are emitted at time t' , where $t = t' + |\vec{R}|/c$ in the case of PXR and $t = t' + |\vec{R}_1|/c$ in the case of CB.

According to Eq. (2), the second derivative of the dipole moment of $\rho_e(\vec{r})dV$ is equal to

$$\delta\ddot{\vec{d}}(\vec{r}, t') = -\frac{e_0}{m_e} \vec{E}(\vec{r}, t') \rho_e(\vec{r}) dV, \quad (4)$$

where m_e is the electron mass. For the dipole radiation caused by this acceleration in the approximation $R_0 \gg r$, where $r = |\vec{r}|$, $R_0 = |\vec{R}_0|$, \vec{r} and \vec{R}_0 are defined in Fig. 1, with $\hat{k} = \vec{R}_0/R_0$ it can be written that

$$\delta\vec{E}(t) = \frac{1}{c^2 R_0} \{[\delta\ddot{\vec{d}}(\vec{r}, t') \times \hat{k}] \times \hat{k}\}. \quad (5)$$

Integrating Eq. (5) over the total crystal volume and taking into account the thermal vibrations of the crystal atoms one obtains for the coherent part of the radiation field,²

$$\begin{aligned} \vec{E}_{PXR}(t) = & \frac{-8\pi z e_0^3}{c^2 V_{cc} m_e R_0 F_D} \\ & \times \sum_{\vec{g}, (\vec{g} \cdot \vec{v} > 0)} \frac{\sqrt{f(\vec{g})} |S(\vec{g})| F(\vec{g})}{(\vec{g} + \vec{k})^2 - k^2} \\ & \times \left\{ \left[\left(\omega \frac{\vec{v}}{c^2} - \vec{g} \right) \times \hat{k} \right] \times \hat{k} \right\} \sin(\phi - \omega t), \quad (6) \end{aligned}$$

where V_{cc} represents the volume of a crystal cell, $f(\vec{g})$ is the Debye-Waller factor, $S(\vec{g})$ the structure factor of a crystal cell, $F(\vec{g})$ the atomic form factor,^{1,2,8} $\omega = \mathcal{E}_{ph}/\hbar$, $\vec{k} = \vec{k}\omega/c$ is a wave vector of the radiated photon, $F_D = 1 - (\vec{v} \cdot \vec{k})/c$, and the summation includes only the reciprocal-lattice vectors satisfying the condition $\vec{g} \cdot \vec{v} > 0$. Each term in the sum corresponds to a single reciprocal-lattice vector of the crystal and describes a single spectral line, the energy of which is defined by Eq. (1). The phase of the radiated electromagnetic wave is given by

$$\phi = \frac{\omega R_0}{c} - \arctan \left(i \frac{S^*(\vec{g}) - S(\vec{g})}{S^*(\vec{g}) + S(\vec{g})} \right). \quad (7)$$

An expression similar to Eq. (6) was derived by Ter-Mikaelian for PXR only, not including the interference with CB.⁸ A quantum-mechanical approach yields the same result.⁹

B. Coherent bremsstrahlung

As already mentioned, due to the interaction between a relativistic charged particle and a crystal, the particle itself is moving with periodical acceleration and thus radiates electromagnetic waves. In general, such radiation is described by the following expression:⁷

$$\vec{E}(t)|_{R_0 \rightarrow \infty} = \frac{ze_0}{c^2 R_0 F_D^3} \left\{ \hat{k} \times \left[\left(\hat{k} - \frac{\vec{v}}{c} \right) \times \frac{d\vec{v}}{dt'} \right]_{t'} \right\}. \quad (8)$$

In the case of CB the acceleration $d\vec{v}/dt'$ is caused by the Coulomb potential of the crystal. A partial acceleration caused by the charge of a small volume of the crystal dV (see Fig. 1) is equal to²

$$\delta \frac{d\vec{v}}{dt'} \Big|_{t'} = [(\vec{r}' \cdot \vec{v}) \vec{v} - \vec{r}' c^2] \frac{ze_0 \rho(\vec{r}) dV}{\gamma m c^2 r'^3}, \quad (9)$$

where m is the rest mass of the relativistic particle, $\rho(\vec{r})$ is a local charge density of the crystal. Inserting Eq. (9) into Eq. (8) and integrating over the total volume of the crystal and taking into account the thermal vibrations of it, for the coherent part of the radiation field one obtains²

$$\begin{aligned} \vec{E}_{CB}(t) &= \frac{-8\pi e_0^3 z^2}{c^2 V_{cc} \gamma m R_0 F_D^2} \\ &\times \sum_{\vec{g}, (\vec{g} \cdot \vec{v}) > 0} |S(\vec{g})| \sqrt{f(\vec{g})} (Z - F(\vec{g})) \cdot \frac{1}{g^2} \\ &\times \left(\left[\left[\omega \frac{\vec{v}}{c} \left(\frac{\hat{k} \cdot \vec{g}}{\vec{g} \cdot \vec{v}} - \frac{1}{c} \right) + \vec{g} \right] \times \hat{k} \right] \times \hat{k} \right) \\ &\times \sin(\phi - \omega t), \end{aligned} \quad (10)$$

where Z is the atomic number of the crystal. This equation can also be expressed in the following form:

$$\begin{aligned} \vec{E}_{CB}(t) &= \frac{-8\pi e_0^3 z^2}{c^2 V_{cc} \gamma m R_0 F_D^2} \\ &\times \sum_{\vec{g}, (\vec{g} \cdot \vec{v}) > 0} |S(\vec{g})| \sqrt{f(\vec{g})} (Z - F(\vec{g})) \cdot \frac{1}{g^2} \\ &\times \left\{ \left[\left(\omega \frac{\vec{v}}{c} \cdot \frac{\hat{k} \cdot \vec{g}'}{\vec{g} \cdot \vec{v}} + \vec{g}' \right) \times \hat{k} \right] \times \hat{k} \right\} \\ &\times \sin(\phi - \omega t), \end{aligned} \quad (11)$$

where $\vec{g}' = \vec{g}_\perp + \vec{g}_\parallel / \gamma^2$, \vec{g}_\perp and \vec{g}_\parallel represent the normal and parallel components of \vec{g} with respect to the velocity \vec{v} of the particle. Applying this expression for the forward direction, i.e., for the case $\hat{k} \parallel \vec{v}$, one obtains $[\vec{g}_\parallel \times \hat{k}] = 0$. In this case Eq. (11) matches with the expressions which are commonly used for the extremely small observation angles.

C. Interference between PXR and CB

From the above it is obvious that both, the crystal and the relativistic particle itself contribute to the radiation field at the observation point (see Fig. 1). The contribution of the crystal is called PXR, its electric-field component is described by Eq. (6). The contribution of the relativistic particle is called CB and is expressed by Eq. (10). Since both expressions are calculated in the same coordinate system the total radiation amplitude is given by the sum of Eqs. (6) and (10):

$$\begin{aligned} \vec{E}_{PXR+CB}(t) &= \vec{E}_{PXR}(t) + \vec{E}_{CB}(t) \\ &= \frac{-8\pi e_0^3}{c^2 V_{cc} R_0 (1 - \vec{v} \cdot \hat{k}/c)} \\ &\times \sum_{\vec{g}, (\vec{g} \cdot \vec{v}) > 0} \sqrt{f(\vec{g})} |S(\vec{g})| \\ &\times \left[\left(\left[\frac{zF(\vec{g})}{m_e [(\vec{g} + \vec{k})^2 - k^2]} \left(\omega \frac{\vec{v}}{c^2} - \vec{g} \right) \right. \right. \right. \\ &\quad \left. \left. \left. + \frac{z^2 [Z - F(\vec{g})]}{\gamma m (1 - \vec{v} \cdot \hat{k}/c) g^2} \right] \right) \times \hat{k} \right] \\ &\times \sin(\phi - \omega t). \end{aligned} \quad (12)$$

The number of photons emitted from a segment dL of the particle trajectory into a solid angle $d\Omega$ can then be expressed as follows:²

$$\begin{aligned} \frac{d^3 N}{dL d\Omega} &= \frac{8\pi e_0^6}{c^3 v \hbar V_{cc}^2} \sum_{\vec{g}, (\vec{g} \cdot \vec{v}) > 0} \frac{|S(\vec{g})|^2 f(\vec{g})}{\vec{g} \cdot \vec{v}} \\ &\times \left[\left(\left[\frac{zF(\vec{g})}{m_e ((\vec{g} + \vec{k})^2 - k^2)} \left(\omega \frac{\vec{v}}{c^2} - \vec{g} \right) \right. \right. \right. \\ &\quad \left. \left. \left. + \frac{z^2 (Z - F(\vec{g}))}{\gamma m (1 - \vec{v} \cdot \hat{k}/c) g^2} \right] \right) \times \hat{k} \right]^2. \end{aligned} \quad (13)$$

The first term inside the brackets corresponds to PXR, the second one to CB.

Using Eq. (13) for 3-MeV electrons and a 55- μm -thick diamond crystal one obtains the angular distribution displayed in form of a polar diagram in Fig. 2. The calculations were performed for a single (111) plane of the crystal, i.e., only one term in the sum has been included, and thus describe a single spectral line. The energy of this line is defined by Eq. (1). The crystal surface is perpendicular to the plane of Fig. 2 and parallel to the reciprocal-lattice vector denoted by $\vec{g}(111)$.

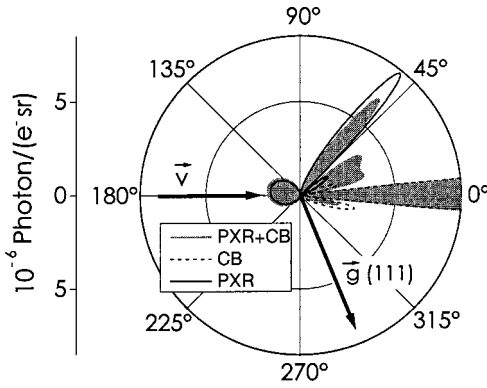


FIG. 2. Angular distribution of the coherent radiation. The dashed line corresponds to CB, the solid one to PXR. The shaded area shows the result of the interference between these different types of radiation.

The solid line in Fig. 2 represents the contribution of PXR [first term inside the brackets of Eq. (13)], the dashed line corresponds to CB [second term inside the brackets of Eq. (13)]. The shaded area indicates the coherent superposition of both types of radiation [both terms in brackets of Eq. (13)]. According to these theoretical predictions destructive interference is expected in the region of the large PXR maximum at about 47° . In the angular region between $1/\gamma \approx 8^\circ$ and $4/\gamma \approx 33^\circ$ constructive interference is predicted.

III. EXPERIMENT

A. Experimental setup

The experiments described in detail in Ref. 2 were performed at the superconducting Darmstadt electron linear accelerator S-DALINAC.¹⁰ The radiation was produced by a 4-MeV electron beam interacting with atoms in the (220) plane of a $20\text{-}\mu\text{m}$ $\langle 111 \rangle$ silicon crystal and was observed at an angle of 44° with respect to the electron-beam axis. The experimental setup is shown in Fig. 3.

The reciprocal-lattice vector \vec{g} of the (220) plane producing the radiation lies in the plane composed by the electron beam axis and the axis of the photon channel and is parallel to the surface of the crystal. The crystal was turned step by step around the ϕ axis and in each position an x-ray spectrum was recorded. For the relative normalization of spectra a secondary-emission monitor (SEM) was used. The SEM has a relative accuracy of 0.2% and is described in Ref. 2. For absolute normalization of the angular distribution a Faraday cup was employed.

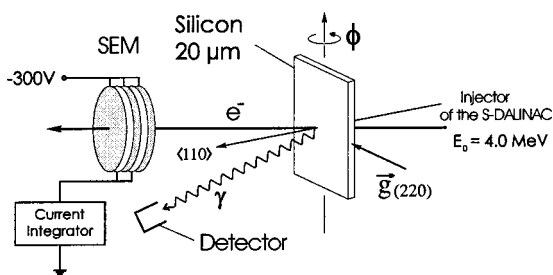


FIG. 3. The experimental setup showing the electron beam, the radiation producing crystal, the x-ray detector, as well as the secondary-emission monitor (SEM).

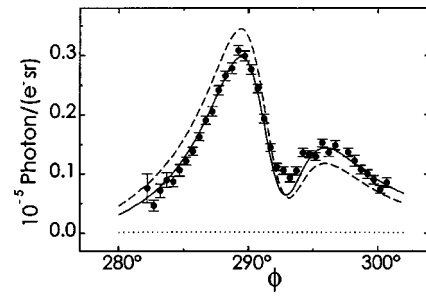


FIG. 4. Angular dependence of the coherent radiation produced by the (220) plane of the $20\text{-}\mu\text{m}$ -thick silicon crystal in comparison with the theory. The data were obtained for electrons with an energy of $E_0 = 4.0$ MeV. The dashed line corresponds to PXR, the dotted line shows the theoretical prediction for CB. The solid line represents the result of the interference between the two types of radiation according to Eq. (13).

B. Results

The number of photons as a function of the rotation angle ϕ obtained from the Si crystal is shown in Fig. 4. The values of ϕ (abscissa in Fig. 4) correspond to the direction of the reciprocal-lattice vector \vec{g} in Fig. 2. The curves represent the theoretical results calculated in absolute units using a Monte Carlo simulation² taking into account effects accomplishing the radiation process as multiple scattering of the relativistic electrons and the absorption of the radiated photons inside the crystal, the finite detector acceptance as well as influence of the initial electron-beam parameters.

The absolute scale in Fig. 4 corresponds to the calculated values, the experimental values were normalized to this scale by multiplying them with a factor of 0.62, which might have been caused by an improper charge collection by the Faraday cup due to a considerable angular spread of the electron beam passing the crystal at this low electron energy. The dashed line represents the predicted contribution of PXR only [first term inside the brackets of Eq. (13)], the dotted line the intensity of CB only [second term of Eq. (13)] and the solid line the interference between both of them [Eq. (13)]. It becomes evident that the experimental points follow the solid line confirming the theoretical predictions of the present paper. Thus the radiation observed results from a

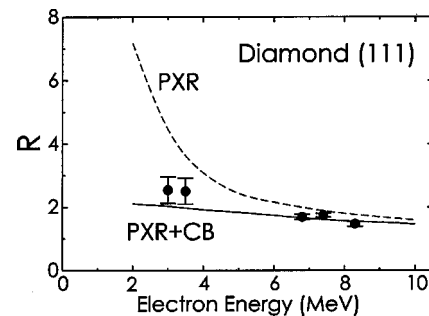


FIG. 5. The ratio R between the first and the second maximum of the angular dependence as a function of the electron energy. The radiation is produced by the atoms in the (111) plane of the $55\text{-}\mu\text{m}$ -thick diamond crystal. The solid line represents the calculation according to Eq. (13). The dashed line corresponds to the contribution of PXR only [first term in the brackets of Eq. (13)].

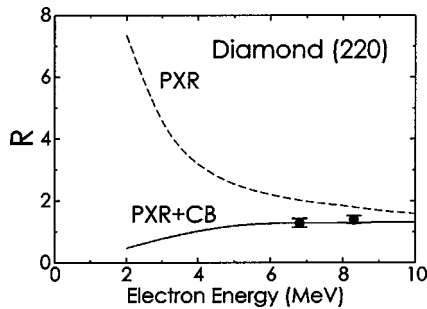


FIG. 6. The ratio R between the first and the second maximum of the angular dependence as a function of the electron energy. The radiation is produced by the atoms in the (220) plane of the 55- μm -thick diamond. The solid line represents the calculation according to Eq. (13). The dashed line corresponds to the contribution of PXR only.

coherent superposition of both types of radiation. It becomes obvious that for the present experimental conditions a tiny amount of CB contribution causes a considerable interference which is destructive at the first maximum of the angular dependence shown in Fig. 4 and constructive at the second maximum.

In order to compare the form of the angular dependence with the theoretical predictions further, the ratio of the intensity at the first maximum and the second one is considered. For the experimental results shown in Fig. 4 the ratio amounts to $R_{EXP} = 2.00 \pm 0.08$. This result agrees perfectly with the theoretical prediction of Eq. (13) (solid line in Fig. 4) yielding $R_{PXR+CB} = 2.05$. The ratio for PXR only, $R_{PXR} = 2.95$, differs strongly from the measured value. The experimental data, obtained at various low energies for different crystals, are presented in the following figures. Figures 5 and 6 show the ratio between the two maxima in the angular dependence of the coherent radiation produced by the (111) and (220) planes of the 55- μm -thick diamond crystal as a function of the electron energy in comparison with the theoretical predictions for PXR (dashed curve) and for the radiation representing a coherent superposition of PXR and CB (solid line). The experimental points in Figs. 5 and 6 result from different experiments performed at the S-DALINAC in the period of 1994–1998.^{2,11} The agreement with the theoretical calculations including the interference is obvious.

Figure 7 shows the comparison between the experimental data published before⁴ and the theory described in the present paper. The experiment⁴ was performed under experimental conditions somewhat different from those at the S-DALINAC. The radiation was produced by the electrons interacting with the (220) plane of a 30- μm -thick silicon crystal and observed at an angle of a 17.5°. The angular dependences were measured at electron energies of 14.49 and 24.49 MeV, respectively. Both experimental data points (full circles) represent the ratio between the first and the second maximum in the angular dependence. The dashed line describes PXR only [first term inside the brackets of Eq. (13)], the solid one takes into account the influence of CB [full expression Eq. (13)]. The diamonds show the theoretical result for PXR only as calculated by the authors of Ref. 4. Inspecting Fig. 7 it becomes evident that the experimental results of Ref. 4 agree very well with the theoretical prediction of the present work, but there is a strong discrepancy

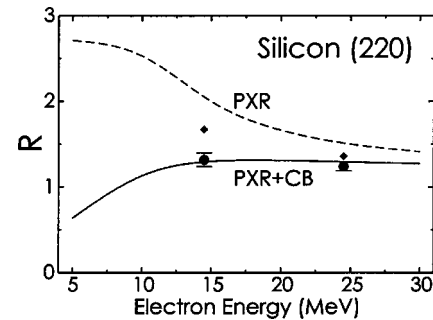


FIG. 7. The ratio R between the first and the second maximum of the angular dependence as a function of the electron energy. The circles show the experimental result of Ref. 4. The solid line was calculated using Eq. (13), the dashed one represents only the first term in brackets of Eq. (13) corresponding to PXR. The diamonds show the theoretical result of Ref. 4 for PXR only, which is in clear disagreement with the predictions of the present paper.

between the theoretical prediction of Ref. 4 for PXR (diamonds) and the theoretical result of the present paper (dashed line). A graphical deduction of the theoretical PXR+CB prediction taken from Fig. 2 of Ref. 4 yields values that coincide with the circles.

Figures 5, 6, and 7 clearly show that the experimental data obtained in the present work and by the authors of Ref. 4 are well described by Eq. (13). It can thus be stated that there exists an interference between PXR and CB.

IV. CONCLUSION

In conclusion it can be stated that interference phenomena between PXR and CB described in the present paper have been verified experimentally. The results of Eq. (13) exhibit very good agreement with all existing experimental data. Even small amounts of CB can cause considerable interference.

For future investigations, the observation of the coherent radiation in the angular region between $1/\gamma$ and $4/\gamma$ is proposed. From Fig. 2 it becomes apparent that the interference in this angular region is most prominent. In this angular region, however, the background caused by incoherent bremsstrahlung will mask the PXR contribution making the experimental determination of the effect difficult if not impossible. Finally it follows from Eq. (13) that the interference term depends on the sign of the charge of the incoming particle. Thus one expects a completely different angular distribution in the case of a positron beam.² In this case, the large PXR maximum should have an increased intensity due to interference.

This research was supported by the Gottlieb Daimler and Carl Benz Stiftung, the Deutsche Forschungsgemeinschaft (DFG) under Contract No. 436UKR113, the Graduiertenkolleg “Physik und Technik von Beschleunigern” from the DFG, and the German Federal Minister for Education and Research (BMBF) under Contract No. 06DA820. The authors wish to thank H.-D. Gräf and his crew for the expert operation of the accelerator.

- *Author to whom correspondence should be addressed. Electronic address: richter@ikp.tu-darmstadt.de
- ¹V. L. Morokhovskii, *The Coherent X-Radiation of Relativistic Electrons in a Crystal* (CSRI atominform, Moscow, 1989), p. 39; an English translation is available from the author upon request.
- ²V. V. Morokhovskiyi, Ph.D. dissertation, Technische Universität Darmstadt, D17, 1998; available from the author upon request.
- ³H. Nitta, Phys. Rev. B **45**, 7621 (1992).
- ⁴S. V. Blazhevich, G. L. Bochek, V. B. Gavrikov, V. I. Kulibaba, N. I. Maslov, N. N. Nasonov, B. H. Pyrogov, A. G. Safronov, and A. V. Torgovkin, Phys. Lett. A **195**, 210 (1994).
- ⁵V. L. Kleiner, N. N. Nasonov, and A. G. Safronov, Phys. Status Solidi B **181**, 223 (1994).
- ⁶D. I. Adejshvili, V. B. Gavrikov, and V. L. Morokhovskii (unpublished).
- ⁷L. D. Landau and E. M. Lifschitz, *Klassische Feldtheorie* (Akademie Verlag GmbH, Berlin, 1992).
- ⁸M. L. Ter-Mikaelian, *High Energy Electromagnetic Processes in Condensed Media* (Wiley, New York, 1972), pp. 332–336.
- ⁹H. Nitta, Phys. Lett. A **158**, 270 (1991).
- ¹⁰A. Richter, *EPAC96, Proceedings of the Fifth EPAC*, edited by S. Myers *et al.* (IOP Publishing, Bristol, 1996), P. 110.
- ¹¹J. Freudenberger, V. B. Gavrikov, M. Galemann, H. Genz, L. Groening, V. L. Morokhovskii, V. V. Morokhovskii, U. Nething, A. Richter, J. P. F. Sellschop, and N. F. Shul'ga, Phys. Rev. Lett. **74**, 2487 (1995).